Synchronization with harmonics in an injected nuclear-magnetic-resonance laser

Yu. V. Pavlov, A. N. Pivkin, R. M. Umarkhodzhaev, and E. G. Lariontsev
Nuclear Physics Institute, Moscow State University, Leninskie Gory, 119992 Moscow, Russia
(Received 25 May 2010; published 8 September 2010)

In injected lasers, only synchronization of the order 1/1 (when a frequency of laser oscillations becomes equal to the master laser frequency) is usually observed. Such locking appears due to single-photon transitions in a laser. We show that with the use of multiple-photon transitions a higher-order synchronization can arise. We present the results of numerical simulations and the preliminary experimental observations, which demonstrate that in the mercury NMR laser, with the use of triple-photon transitions, a frequency of locked laser oscillations becomes three times higher than the frequency of an external rf magnetic field. Such synchronization appears only in the case of a linearly polarized (oscillating) external magnetic field. For the circularly polarized (rotating) external field, only synchronization of the order 1/1 is possible.

DOI: 10.1103/PhysRevA.82.033802 PACS number(s): 42.55.Ah, 42.60.Fc, 05.45.Xt, 42.65.Ky

I. INTRODUCTION

Injection locking of laser oscillations may be considered one of numerous examples of synchronization of self-sustained oscillations by external force. If the frequency of the external force (injected signal) Ω is close to the frequency of the autonomous oscillator (the slave laser) ω_0, one can observe frequency locking (synchronization of the order 1/1). In this case the frequency of forced oscillations ω becomes equal to the frequency of external force ($\omega = \Omega$). In a general case of synchronization of the order n/m (see, for example, [1]), one has the following relation between the frequency of forced oscillations ω and the frequency of an external force Ω:

$$n\omega = m\Omega, \tag{1}$$

where n and m are integers.

Such locking ranges are often called the Arnold tongues [2].

Injection locking of laser oscillations has been studied practically since the invention of the first laser, but in the vast majority of publications on this subject synchronization of an order higher than 1/1 has never been observed in injected lasers (in practically all studies the frequency of the master laser Ω was close to the frequency of an autonomous slave laser ω_0). As one of exclusions, it is worth citing Ref. [3], where injection locking in a solid-state laser with intracavity second-harmonic generation was studied theoretically. As was shown in [3], one can realize, in this case, synchronization of the order 2/1 of laser oscillations, using an injected light with the frequency close to $2\omega_0$.

Apart from synchronization of laser oscillations at the frequencies of the order of ω_0 (the frequency of a resonant quantum transition), there are some publications (see, for example, [4–6]) relating to the high-order synchronization of the self-pulsing oscillations in lasers with feedback. The frequencies of the self-pulsing oscillations and modulating signals, in this case, are much less than ω_0. For such low-frequency oscillations, the high-order synchronization easily appears, and corresponding Arnold tongues were observed in the periodically modulated lasers with optical feedback [4–6]. In a nuclear magnetic resonance (NMR) laser, numerous Arnold tongues, corresponding to such a low-frequency synchronization, were also experimentally observed [7]. With respect to synchronization at frequencies of the order of the frequency of a resonant quantum transition ω_0, only a synchronization of the order 1/1 was observed in the injected ruby NMR laser [8,9].

In contrast with [4–9], we study in this article a higher-order synchronization of laser oscillations by injected signals with frequencies close to ω_0/q, where ω_0 is the frequency of a resonant quantum transition and q is an odd integer. In addition to well-known applications of optical injection for synchronization of optical oscillations, realization of the higher-order synchronization could give a new potential for nonlinear transformation of frequencies of laser oscillations.

In a NMR laser, there is a possibility to use multiple-photon transitions [10,11] for the high-order synchronization of laser oscillations by an injected signal. Such a possibility is discussed in the present article in detail.

This article is structured as follows. In Sec. II we describe the mercury NMR laser with nonresonant feedback and external rf magnetic field. The optical Bloch equations, modified to incorporate nonresonant feedback, are also given in this section. In Secs. III and IV we present the results of numerical simulation and the experimental results concerning of synchronization in the considered system, before drawing our conclusions in Sec. V.

II. MERCURY NMR LASER

For the study of locking phenomena, we choose the mercury (NMR) laser with nonresonant feedback. The mercury NMR-laser activity is produced by the nuclear spins of the mercury isotope ^{199}Hg ($I = 1/2$). For the mercury atoms in the gas phase, optical pumping of nuclear magnetization and optical NMR detection are used. With such a NMR laser, an attempt to search a new type of fundamental interaction (the arion long-range interaction) was performed in [12].

Figure 1 shows a schematic of the experimental setup. For simplicity, in Fig. 1 we show only one feedback circuit (for H_x). The sample is a quartz cell containing the vapors of atoms of the mercury isotope ^{199}Hg at a pressure of 10^{-3} Torr. The mercury atoms are subjected to a static external magnetic field H_0, which is provided by a solenoid L_z and is parallel to the z axis. The x and y axes are parallel to the axes of two feedback coils L_x and L_y.

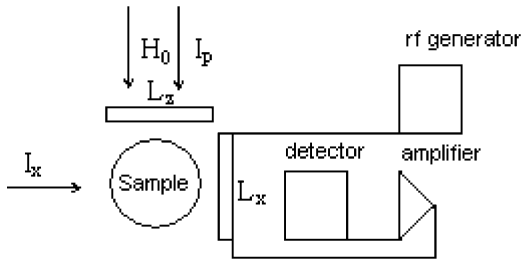

FIG. 1. Schematic of the mercury NMR laser with nonresonant feedback and external rf magnetic field.

Nuclear magnetization in the mercury NMR laser is optically pumped by a resonant light at 2537 Å, which is produced by a spectral lamp with the isotope ^{204}Hg. The light beam for optical pumping I_p has circular polarization and is parallel to the direction of magnetic field H_0. The linearly polarized nonresonant light beams I_x and I_y for optical NMR detection are perpendicular to $\vec{H}_0$ and parallel to the x and y axes. Due to the Faraday effect [13], precession of transverse nuclear magnetization $M_{x,y}$ with the frequency ω creates the rotation of the polarization of the monitoring light beams $I_{x,y}$. This rotation, proportional to $M_{x,y}$, is transformed into modulation of the intensities $I_{x,y}$ after passing the analyzers (not shown in Fig. 1), which are placed before the photodetectors. After detection of the monitoring beams, two rf signals with the frequency ω appear on the photodetectors. These signals are amplified by the broadband rf amplifiers and produce transverse magnetic fields $H_{x,y}$ of feedback. The magnetic fields $H_{x,y}$ are proportional to the currents $I_{x,y}$ in the feedback coils $L_{x,y}$.

The main difference of this NMR laser from the ruby NMR laser studied in Refs. [7–9] is the following. In the ruby NMR laser a LC circuit with a resonance frequency $\omega_{=}1/\sqrt{LC}$ plays the role of the cavity of a laser. In the mercury NMR laser, feedback is nonresonant. The feedback circuits of the mercury NMR laser include two photodetectors, two broadband linear rf amplifiers, and the feedback coils $L_{x,y}$. The mercury NMR laser can be driven by an injected signal.

In the presence of injected signal, one can write transverse magnetic fields $H_{x,y}$ as

$$H_x = K_x M_y + H_x^{\text{ext}} \cos \Omega t, \quad H_y = K_y M_x + H_y^{\text{ext}} \sin \Omega t, \tag{2}$$

where $K_{x,y}$ are the transmission coefficients in the corresponding feedback circuits and $H_x^{\text{ext}} \cos \Omega t$ and $H_y^{\text{ext}} \sin \Omega t$ are the external magnetic fields produced by the rf generator.

The dynamical variables of the mercury NMR laser are the components (H_x, H_y) of the precessing magnetic rf field in the feedback coils $L_{x,y}$, the components (M_x, M_y) of the precessing transverse nuclear magnetization, and the longitudinal nuclear magnetization M_z. We may model the mercury NMR laser using the so-called Bloch-Kirchhoff equations,

$$d\vec{M}/dt = \gamma[\vec{M}\vec{H}] - \vec{e}_x \frac{1}{T_2} M_x - \vec{e}_y \frac{1}{T_2} M_y + \vec{e}_z \frac{1}{T_1}(M_0 - M_z), \tag{3}$$

where $\vec{e}_{x,y,z}$ are the unit vectors in the directions x, y, z, γ is the gyromagnetic ratio of the ^{199}Hg spins, T_2 is the transverse relaxation time, $1/T_1$ is an effective pump rate, and M_0 is magnetization produced by optical pump. Nonresonant feedback and the external rf signal are described in the mercury NMR laser by relations (2).

For numerical simulations, it is convenient to rewrite Eqs. (3) with account of (2) in the dimensionless form

$$\begin{cases} dx/d\tau + x(1 - \kappa_y z) = \alpha y + b_y z \sin \bar{\Omega}\tau, \\ dy/d\tau + y(1 - \kappa_x z) = -\alpha x + b_x z \cos \bar{\Omega}\tau, \\ dz/d\tau + zr = -\kappa_y x^2 - \kappa_x y^2 - b_x y \cos \bar{\Omega}\tau - b_y x \sin \bar{\Omega}\tau + r, \end{cases} \tag{4}$$

where $x = \frac{M_x}{M_0}$, $y = \frac{M_y}{M_0}$, $z = \frac{M_z}{M_0}$, $\tau = t/T_2$, and

$$\kappa_{x,y} = K_{x,y}\gamma M_0 T_2, \quad \alpha = \omega_0 T_2, \quad b_{x,y} = \gamma H_{x,y}^{\text{ext}} T_2, \quad \bar{\Omega} = \Omega T_2, r = T_2/T_1. \tag{5}$$

In (5) we denote $\omega_0 = \gamma H_0$, where ω_0 is the central frequency of the NMR transition.

Equations (4) were used for the simulations and analytical studies presented in what follows. In these investigations, frequency locking of the mercury NMR laser by an external rf magnetic field was considered. With the use of triple-photon transitions [10,11], synchronization of the order $1/3$, when the frequency Ω was close to $\omega_0/3$, was, at first, discovered in these simulations and in preliminary experimental investigations.

III. LOCKED STATES INDUCED BY EXTERNAL RF MAGNETIC FIELD

In what follows we present the results of theoretical study and numerical simulations for the mercury NMR laser in the presence of an external rf magnetic field. We consider two types of an external rf magnetic field: the circularly polarized (rotating) external field and the linearly polarized (oscillating) external field.

A. Rotating external field

In the case of a rotating external field ($H_x^{\text{ext}} = H_y^{\text{ext}} = H_\perp$, $b_x = b_y = b = \gamma H_\perp T_2$, $k_x = k_y = k$), one can find analytically an exact periodic solution of Eqs. (4) for the locked state. This solution is the following:

$$x = A \sin(\bar{\Omega}\tau) + B \cos(\bar{\Omega}\tau), \quad y = -B \sin(\bar{\Omega}\tau) + A \cos(\bar{\Omega}\tau), \quad z = C = \text{const}, \tag{6}$$

where $A = \frac{bC(1-kC)}{(\alpha-\bar{\Omega})^2+(1-kC)^2}$, $B = \frac{bC(\alpha-\bar{\Omega})}{(\alpha-\bar{\Omega})^2+(1-kC)^2}$, and C is a root of the cubic equation

$$(C-1)r[(\alpha - \bar{\Omega})^2 + (1 - kC)^2] + b^2 C = 0. \tag{7}$$

This solution is stable if $kC < 1$. The stability condition $kC < 1$ is fulfilled inside the locking range, $\Omega_- \leqslant \Omega \leqslant \Omega_+$, and the boundaries of the locking range are determined by the condition $kC = 1$. After substitution $C = 1/k$ in Eq. (6), one finds the following expressions for the left (Ω_-) and right (Ω_+) boundaries of the locking range:

$$(\Omega_\pm - \omega_0)/\omega_0 \equiv (\bar{\Omega}_\pm - \alpha)/\alpha = \pm b/[\alpha\sqrt{(k-1)r}]. \tag{8}$$

Using (5) one can rewrite (8) as

$$(\Omega_\pm - \omega_0)/\omega_0 = \pm(H_\perp/H_0)/\sqrt{(k-1)r}. \tag{9}$$

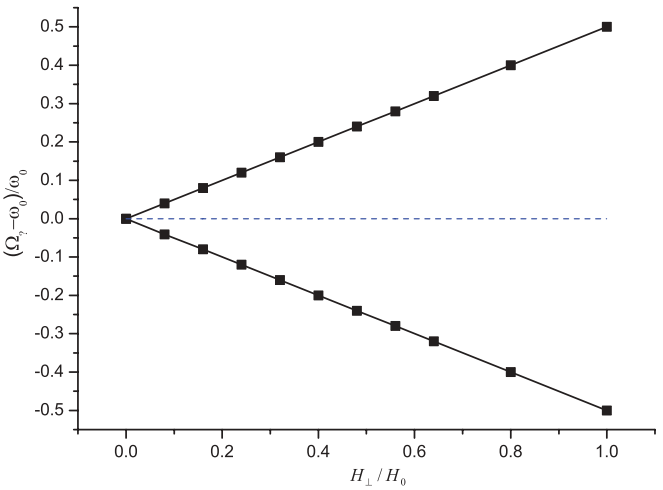

FIG. 2. (Color online) The left (Ω_-) and right (Ω_+) boundaries of the locking range 1/1 in units of the central frequency of the laser transition, $\omega_0 = \gamma H_0$, versus the ratio of the amplitude $H_\perp$ of a circularly polarized (rotating) external rf magnetic field to the strength of a static magnetic field H_0. The solid lines show the analytical results given by (9). The squares are the results of numerical simulations. The dashed line corresponds to the resonant frequency ($\Omega = \omega_0$).

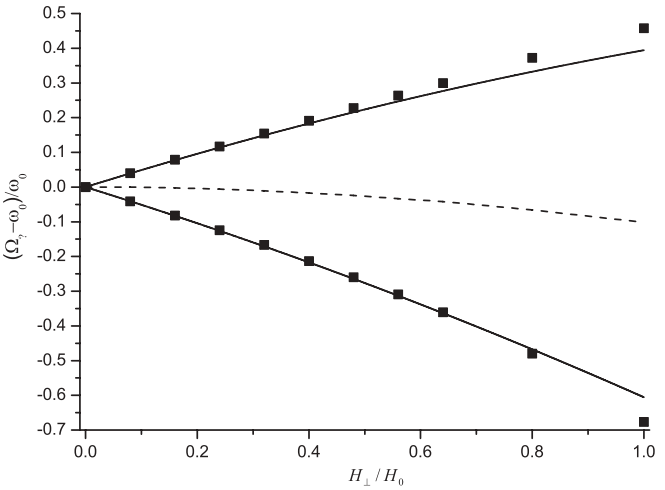

FIG. 3. The same as in Fig. 2, but in the case of a linearly polarized (oscillating) external rf magnetic field. The solid lines correspond to the approximations given by (11), and the dashed curve corresponds to the shifted resonant frequency [see (10)].

It follows from (9) that the width $\Omega_+ - \Omega_-$ of the locking range of the order 1/1 is proportional to the amplitude $H_\perp$ of the external magnetic field.

We have solved numerically Eqs. (4) for the following values of laser parameters: $r = 1 (T_1 = T_2)$, $k_x = k_y = k = 2$, $\alpha = 100$. The results of numerical simulations (see Fig. 2) are in excellent agreement with the analytical results given by (9). Numerical simulations have shown that for the circularly polarized external magnetic field only a synchronization of the order 1/1 might be observed. In this case only a main resonance (at $\omega_0 \approx \Omega$) exists and higher-order resonances at $\omega_0 \approx (2m+1)\Omega$($m$ is integer) disappear. The NMR laser with the circularly polarized magnetic field is an isochronous self-oscillation system: The Bloch-Siegert shift of the resonant frequency [14] is absent in this case, and the frequency of laser oscillations ω does not depend on their amplitude ($\omega = \omega_0 = \gamma H_0$). Due to isochronisms, the boundaries of the locking range [see (9) and Fig. 2] are symmetric about the central line $\Omega - \omega_0 = 0$. The Arnold tongues corresponding to synchronization of a higher order were found only for the oscillating (linearly polarized) external field.

B. Oscillating external field

For the oscillating external magnetic fields ($H_x^{\text{ext}} = H_\perp$, $H_y^{\text{ext}} = 0$, $b_x = \gamma H_\perp T_2$, $b_y = 0$), Eqs. (4) were numerically solved by us at the same values of parameters: $r = 1 (T_1 = T_2)$, $k_x = k_y = 2$, $\alpha = 100$.

In numerical simulations we have observed the Arnold tongue (synchronization of the order 1/1) with the use of single-photon transitions (Fig. 3). This Arnold tongue is analogous to that one for the circularly polarized external magnetic field (Fig. 2) but the boundaries of the locking range are here nonsymmetric about the line $\Omega - \omega_0 = 0$. In this case the Bloch-Siegert shift of the resonant frequency [14] is observed: The shifted resonant frequency ω is equal to

$$\omega = \omega_0 - \gamma H_\perp^2 / 16 H_0. \tag{10}$$

The results of numerical simulations show that the left (Ω_-) and right (Ω_+) boundaries of the locking range may be approximated (at the parameters used in this numerical simulation) by the expressions

$$(\Omega_\pm - \omega_0)/\omega_0 = -(1.3 H_\perp / 4 H_0)^2 \pm H_\perp / 2 H_0, \tag{11}$$

when $H_\perp \ll H_0$. It follows from (11) that the width $\Omega_+ - \Omega_-$ of the locking range of the order 1/1 is proportional to the amplitude $H_\perp$ for weak external magnetic fields (when $H_\perp \ll H_0$):

$$(\Omega_+ - \Omega_-)/\omega_0 = H_\perp / H_0. \tag{12}$$

In addition to the main resonance ($\omega_0 \approx \Omega$), the higher-order resonances at $\omega_0 \approx (2m+1)\Omega$($m$ is integer) appear due to multiple-photon transitions [10,11]. In numerical simulations we have observed the Arnold tongue (synchronization of the order 1/3) with the use of the triple-photon transition (Fig. 4). For a triple-photon transition ($\omega_0 \approx 3\Omega$), the shifted resonant frequency is equal to [10]

$$\omega = \omega_0 - 9\gamma H_\perp^2 / 32 H_0. \tag{13}$$

As consistent with the results of numerical simulations, the left (Ω_-) and right (Ω_+) boundaries of the locking range may be approximated, at the parameters used in the simulations, by the expressions

$$(3\Omega_\pm - \omega_0)/\omega_0 = (3 H_\perp / 4 H_0)^2 / 2 \pm (H_\perp / H_0)^3 / 9 \tag{14}$$

for $H_\perp \ll H_0$.

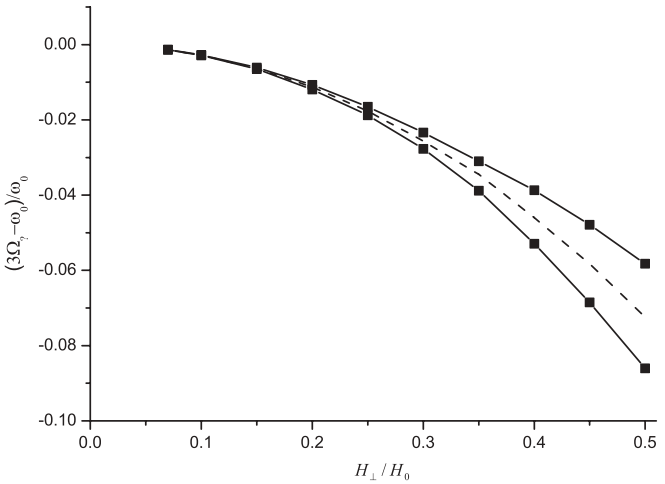

FIG. 4. The left $(3\Omega_-)$ and right $(3\Omega_+)$ boundaries of the locking range 1/3 in units of a central frequency of the laser transition, $\omega_0 = \gamma H_0$, versus the ratio of the amplitude $H_\perp$ of a linearly polarized (oscillating) external rf magnetic field to the strength of a static magnetic field H_0. The solid lines correspond to the approximations given by (14). The dashed curve corresponds to the shifted resonant frequency [$3\Omega = \omega$, see (13) and (14)].

As follows from (14), the width $\Omega_+ - \Omega_-$ of the locking range of the order 1/3 is proportional, for $H_\perp \ll H_0$, to the cube of the amplitude $H_\perp$:

$$3(\Omega_+ - \Omega_-)/\omega_0 = 2(H_\perp/H_0)^3/9. \qquad (15)$$

IV. EXPERIMENTAL RESULTS

The Arnold tongues 1/1 and 1/3 were observed by us experimentally for the linearly polarized (oscillating) external rf magnetic field. In the NMR laser under study, the central frequency of laser transition was $\omega_0/2\pi = 10^4$ Hz. In Fig. 5 we show the experimentally measured dependence of the locking-range width of the order 1/1 on the amplitude $H_\perp$ of the external magnetic field. It was difficult to measure the effective amplitude $H_\perp$ since the external magnetic field is applied to the nuclear spins placed inside the quartz cell. Using this reason, we give in Figs. 5 and 6 the values of $H_\perp$ in arbitrary units. Experimental investigations show (see Fig. 5) that, in accordance with the theory, the width of the locking range 1/1 is proportional to $H_\perp$. Using the autonomous slave laser frequency $\omega_0/2\pi = 10^4$ Hz, it is possible to estimate $H_\perp$ comparing the experimental results in Fig. 5 with the expression (12). For the measured width of the locking range $(\Omega_+ - \Omega_-)/2\pi = 100$ Hz, one obtains $H_\perp/H_0 = 0{,}01$.

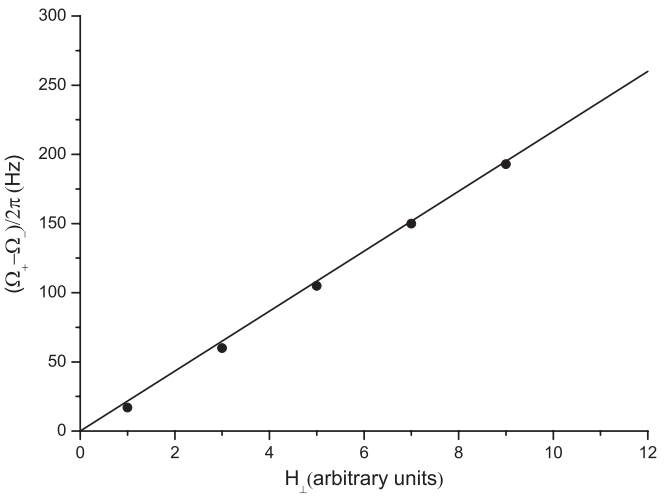

FIG. 5. Measured width of the locking range 1/1 versus the amplitude $H_\perp$ of a linearly polarized (oscillating) rf magnetic field. The solid line corresponds to the equation $(\Omega_+ - \Omega_-)/2\pi = 22H_\perp$ [see (12)].

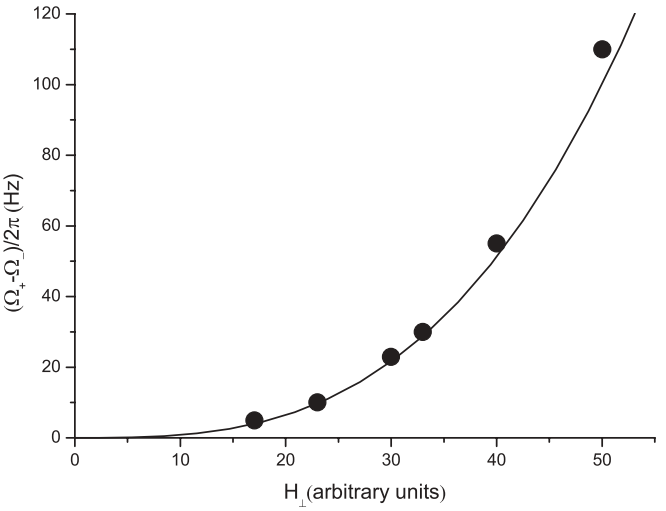

FIG. 6. Measured width of the locking range 1/3 versus the amplitude $H_\perp$ of a linearly polarized (oscillating) rf magnetic field. The solid line corresponds to the equation $(\Omega_+ - \Omega_-)/2\pi = 9 \times 10^{-4} H_\perp^3$ [see (15)].

Figure 6 shows the experimentally measured dependence of the locking-range width of the order 1/3 on the amplitude $H_\perp$ of the external magnetic field. In accordance with theory, the experimentally measured width of this locking range is proportional to cube of $H_\perp$ for weak external magnetic fields (when $H_\perp \ll H_0$). Comparing the experimental results in Fig. 6 with the expression (15), we estimate $H_\perp/H_0 = 0{,}5$ for the measured width of the locking range $(\Omega_+ - \Omega_-)/2\pi = 100$ Hz.

V. CONCLUSION

In summary, we have demonstrated numerically and experimentally that, with the use of triple-photon transitions, the frequency of locked oscillations of the mercury NMR laser is three times higher than the frequency of an external rf magnetic field. The Arnold tongues 1/1 and 1/3 are observed in the case of a linearly polarized (oscillating) external magnetic field. For a circularly polarized external field, only synchronization of the order 1/1 is possible. For weak external magnetic fields ($H_\perp \ll H_0$), the locking-range width of the order 1/1 is proportional to the amplitude $H_\perp$ of the external magnetic field, and that of the order 1/3 is proportional to the cube of $H_\perp$.

ACKNOWLEDGMENTS

We thank N.V. Kravtsov for discussion. E.G.L. acknowledges the support of the Russian Foundation for Basic Research (Grant No. 10-02-00453 a).

[1] A. Pikovsky, M. Rosenblum, and J. Kurtz, *Synchronization: A Universal Concept in Nonlinear Sciences* (Cambrige University Press, Cambridge, 2003).
[2] V. I. Arnold, *Mathematical Methods of Classical Mechanics* (Springer-Verlag, Berlin, 1989).
[3] I. I. Zolotoverkh and E. G. Lariontsev, Quantum Electron. **30**, 787 (2000).
[4] J. Sacher, D. Baums, P. Panknin, W. Elsasser, and E. O. Gobel, Phys. Rev. A **45**, 1893 (1992).
[5] J. M. Mendez, R. Laje, M. Giudici, J. Aliaga, and G. B. Mindlin, Phys. Rev. E **63**, 066218 (2001).
[6] F. R. Ruiz-Oliveras and A. N. Pisarchik, Opt. Express **14**, 12859 (2006).
[7] J. Simonet, M. Warden, and E. Brun, Phys. Rev. E **50**, 3383 (1994).
[8] E. Brun, B. Derighetti, D. Meier, R. Holzner, and M. Ravani, J. Opt. Soc. Am. B **2**, 156 (1985).
[9] E. Brun, B. Derighetti, M. Ravani, G. Broggi, P. Meier, R. Stopp, and R. Badii, Phys. Scr., T **13**, 119 (1986).
[10] J. H. Shirley, Phys. Rev. **138**, 979 (1965).
[11] S. Stenholm, J. Phys. B **5**, 878 (1972).
[12] E. B. Aleksandrov, A. A. Ansel'm, Yu. V. Pavlov, and R. M. Umarkhodzhaev, Sov. Phys. JETP **58**, 1107 (1983).
[13] J. Manuel and J. C. Cohen-Tannoudji, Compt. Rend. B **257**, 413 (1963).
[14] F. Bloch and A. Siegert, Phys. Rev. **57**, 522 (1940).